Air Gasification of Dried Sewage Sludge in a Fluidized Bed: Effect of the Operating Conditions and In-Bed Use of Alumina

Joan J. Manyà[*]*, José L. Sánchez, Alberto Gonzalo, and Jesús Arauzo*

Thermo-chemical Processes Group (GPT), Aragón Institute of Engineering Research (I3A), University of Zaragoza, Maria de Luna 3, E-50018 Zaragoza, Spain.

[*] Corresponding author. Tel: +34-976-762224. Fax: +34-976-761879. E-mail: joanjoma@unizar.es

Abstract

Sewage sludge has recently become a particularly important problem all over the world because of its harmful impact on the environment. The consequent need to develop alternative processes for the use of dried sewage sludge for energy purposes, such as gasification, requires experimental tests in order to quantify the potential energy power of the sludge as well as to evaluate the optimum conditions for its gasification. There is, however, little information available. In this study, the gasification with air of dried sewage sludge was experimentally investigated using a bubbling fluidized bed. Attention was focused on the influence of the temperature (750–850 ºC), the equivalence ratio (25–35 %), and the fluidizing velocity (5, 8, and 11 times the value of u_{mf}) on the product yields, gas composition, thermal efficiency, and tar content. The results obtained show the potential for using sewage sludge gasification with air as an option for energy recovery and waste treatment. However, the high tar yield obtained needs to be reduced. Consequently, experiments involving the in-bed use of alumina were carried out. This primary measure has proven effective for tar removal (the content decreases by nearly 40 % with in-bed use of alumina at 5 wt %).

Keywords

Sewage sludge; Gasification; Bubbling Fluidized Bed; Bed additive; Tar removal

Introduction

Sewage sludge is the residue produced by the treatment of domestic and industrial waste-waters. The rate of production in the European Union (EU) is forecast to increase to approximately 10 Mton/year (dry basis) by 2005,[1] and will probably increase further as municipal waste-water treatment plants are continually being built to comply with environmental standards.[2] The costs of disposal and treatment of sewage sludge may be up to 50 % of the total waste-water treatment cost.[3]

The most common methods of treatment and/or disposal of sewage sludge are land filling, cropland application and incineration, none of which are exempt from drawbacks.[1] It is important to develop a technology for the appropriate treatment of sewage sludge in order to reduce environmental problems and costs.

Researchers interested in sewage sludge have studied its pyrolysis since 1980.[4-9] In addition, several researchers have investigated its drying properties[10] and production from the sludge of fuel and chemical matter.[11-13] The properties of pyrolysis coke from sewage sludge and its possible applications[14] and the combustion of sewage sludge with heat recovery[15] have also been investigated. It can be assumed that gasification is a suitable technology because it reduces waste volume, removes toxic organic compounds and fixes heavy metals in the resultant solid.[16]

The gasification process converts any carbon containing material into a combustible gas composed primarily of carbon monoxide, hydrogen, methane, and nitrogen (if air is used as gasifying agent), which can be used as a fuel to generate electricity and heat. Part of these gases can be used to dry wet sewage sludge. However, one of the major issues in biomass gasification is to deal with the tar formed during the process. Tar is a complex mixture of condensable hydrocarbons, which includes single ring to 5-ring

aromatic compounds along with other oxygen-containing hydrocarbons and complex PAH.[17]

Tar is undesirable because of various problems associated with condensation, formation of tar aerosols, and polymerization to form more complex structures, all of which cause problems in the process equipment as well as in the engines and turbines used in application of producer gas. However, the minimum allowable limit for tar is highly dependent on the kind of process and the end user application.

Considerable efforts have been directed towards tar removal from fuel gas. Tar removal technologies can broadly be divided into two approaches: treatments inside the gasifier (primary methods), aimed at the production of a gas as free of tar as possible, and gas cleaning after the gasifier (secondary methods).[18] The secondary methods can consist of a hot gas clean-up, usually catalytic or thermal tar cracking (which can enrich the gas energy content) or simply tar removal from the cold gas by means of wet scrubbers or electrostatic precipitators.[19] Although hot secondary methods are proven to be effective,[20,21] treatments inside the gasifier are gaining much attention as these may eliminate the need for downstream cleanup. In primary treatment, the gasifier should be optimized in order to produce a fuel gas with minimum tar concentration.

In this work, the use of a laboratory scale, atmospheric bubbling fluidized bed reactor to gasify dried sewage sludge with air (using sand as bed material), has been studied. The goal of the present study is to evaluate the performance of the process. Because of the high level of volatiles in the sewage-based material, there is a potential for high concentrations of tar in the fuel gas. However, the amount of tar remaining in the gas leaving the gasifier will depend on the operating conditions (i.e. temperature, pressure, equivalence ratio, residence time, bed height, nature of the bed material, etc.). Little

information is available on how these parameters affect the nature and concentration of tar formed during the gasification of sewage sludge.

Experiments involving treatment inside the gasifier, using alumina as additive, have been carried out. The goal of these experiments is to evaluate the efficiency of the addition of alumina as a primary measure for tar removal.

Experimental Section

BFB Reactor Facility. Experiments have been carried out in a laboratory scale plant operating at atmospheric pressure, continuously feeding sewage sludge and air, and with a continuous ash removal system. The plant is coupled to a gas cleaning system. Figure 1 shows a diagram of the system.

The reactor is made of refractory steel (AISI 310), with an inner diameter of 38.1 mm and a height of 800 mm. Biomass is fed through a sloping pipe (13.1 mm inner diameter), provided with an air jacket to avoid pyrolysis before entering the reactor. The bed height is kept at 150 mm during the experiment by a concentric pipe (13.1 mm inner diameter) which goes through the distributor plate, enabling the bed material to overflow and be collected in an ash hopper.

The reactor is heated by an electrical furnace, with three independent heating zones (bed, freeboard, and cyclone). Biomass is fed by a variable speed screw feeder, and the air flow rate is set by a mass flow controller. About 33 % of the gasification air is diverted to the screw feeder, thus helping the solid to enter the reactor, while the other 67 % enters the reactor through the distributor plate.

After the reactor a small cyclone removes particles entrained by the gas produced, which are collected in a “char pot”.

The gas leaving the cyclone is cooled in two ice condensers, where most of the tar and water are collected. The tar and water are extracted with 2-propanol, and the water is determined off-line using a Karl Fischer titration (tar is calculated by difference). Final cleaning of the gas is performed by a cotton filter. Part of the cleaned gas is diverted to a continuous CO/CO_2 infrared analyzer, which is used to monitor the process.

Gas production is measured by a volumetric gas meter, taking into account gas temperature and pressure. The gas composition is determined by means of a micro gas chromatograph (Agilent 3000A) connected on-line to the process, giving the volume percentage of N_2, O_2, H_2, CO, CO_2, CH_4, C_2H_2, C_2H_4, C_2H_6, and H_2S. The time interval between two consecutive analyses is approximately 4 min.

Materials. The samples of dry sewage sludge (DSS) used in the study were obtained as a dried, granulate product from an urban waste-water treatment plant. The sludge was previously treated by anaerobic digestion and thermal drying. Proximate and ultimate analyses of the received sewage sludge are shown in Table 1. The lower heating value (LHV) has also been determined using a calorimeter IKA A-2000 (standard procedure: ISO-1928-89). The value obtained for LHV is 10.26 MJ/kg. All analyses were performed by the Instituto de Carboquímica (CSIC, Zaragoza, Spain). The dried sewage sludge was crushed and sieved to provide a feed sample in the size range of 250–500 μm.

For the catalytic experiments, a mixture of sand and activated alumina (Spheralite 505) supplied by Axens Procatalyse Catalysts & Adsorbents was used as bed material. The catalyst was received in spherical pellet form. The pellets were crushed and sieved to the same size as the dry sewage sludge and sand (250–500 μm). Table 2 summarizes some of the physical and chemical properties of the catalyst.

Experimental Procedure. The laboratory experiments are grouped into three sections:

- Section I: Initial gasification experiments performed in order to check the influence of the temperature and the equivalence ratio on the process.
- Section II: Additional experiments varying the fluidizing velocity.
- Section III: Gasification experiments using alumina as bed additive. The catalyst is mixed with sand in different proportions.

Table 3 shows the scheduled operating conditions for all experiments performed.

The initial gasification experiments were performed at three different temperatures (750, 800, and 850 ºC) and at three different values of the equivalence ratio, λ, (25, 30, and 35 %), defined as the ratio between the actual flow rate of the air and the stoichiometric flow rate required for fuel combustion.

The hopper was filled with sewage sludge and a sand/alumina mixture (20 % of the mass rate of DSS). The sand and alumina proportion for each experiment is shown in Table 3 . Previously to perform an experimental run, the reactor was loaded with 50 g of bed material (a sand/alumina mixture at the same proportion as reported in Table 3) in the size fraction of 250–500 μm (u_{mf} = 2.8 ± 0.1 cm s^{-1} at 850 ºC).

In order to calculate the amount of air needed for stoichiometric combustion of the residue, the carbon, hydrogen, and sulfur contents were considered. It was found that 3.31 × 10^{-3} m_0^3 of air per gram of residue were necessary for complete combustion. Thus, the air ratio used in an experiment can be calculated as follows:

$$\lambda = \frac{Q_{air}}{Q_{sludge} \times 3.31} \times 100 \quad (1)$$

where Q_{air} is the air flow rate used in an experiment (l_0/min), and Q_{sludge} is the mass flow rate of sewage sludge (g/min). The value of Q_{air}, flowing at eight times the minimum fluidizing velocity, was fixed at 3.75 l_0/min. In this way, the value of the λ

was changed adjusting the feed rate of solid. The average experiment length was 45 minutes.

Results and Discussion

The results presented in this paper show the influence of the operating conditions on gasification efficiency. Moreover, the influence of alumina addition on tar removal has been studied.

Influence of the operating conditions. Table 4 reports the results of gasification tests corresponding to sections I and II (see Table 3). The data presented for each experiment correspond to: the experimental equivalence ratio, experimental biomass flow rate, average gas composition (dry basis), the specific yield to gas obtained (y_{gas}), the lower heating value of the gas (LHV), the average cold gas efficiency defined as the ratio of the LHV of the produced gas to the LHV of the DSS fed (η), the average percentage of carbon in the biomass recovered in the gas (y_{carbon}), and the mass product distribution. The product distribution is shown based on the biomass fed and also on the DSS weight plus the air mass fed during the experiment, giving an experiment closure of nearly 100 %.

In order to check the reproducibility of experimental results, two repetitions of run #I.6 were carried out (runs #I.6b and #I.6c). The results shown in Table 5 confirm that experimental error was not critical.

Figure 2 shows the evolution of the gas composition during an experiment. Changes in the composition of CO, CO_2, and H_2 were observed (the composition of the rest of the components remains practically constant). This effect was typically observed in all the experiments performed and could be caused by the change in bed composition

during the run which at the start is composed of sand and during the experiment is replaced by a mixture of sand and char. This result confirms the stability of the plant.

Regarding the quality of the product gas, the lower heating value was only 3–4 MJ/m_0^3 (see Table 4) compared to typically 5 MJ/m_0^3 corresponding to gasification from wood. Also, the feed carbon to gas conversion (y_{carbon}) was 50–75 %, much less than for other biomass feedstocks. One possible explanation for these results could be related to the fact that the high ash content of DSS represents an obstacle to the gas diffusion. As a consequence, the intrinsic kinetics of the particle conversion is lower than for low-ash fuels.

Figure 3 shows the average gas composition of the exit gas as a function of temperature and equivalence ratio (experiments I.1–I.9). Furthermore, the evolution of the LHV of the exit gas and the average cold gas efficiency (η) as a function of both *T* and λ values are also shown, respectively, in Figure 4 and Figure 5. As can be seen, both LHV and η increase with the temperature. The increase of LHV with temperature (observed for each value of equivalence ratio) can be attributed to steam reforming (generation of H_2 and CO) and steam cracking reactions (generation of H_2 and light hydrocarbons). This double effect could compensate the decrease of the production of light hydrocarbons from DSS thermal decomposition. However, some observations should be made about the influence of the equivalence ratio. The lower heating value of the gas produced decreases with λ only at 850 ºC. Below this temperature, Figure 4 does not show a clear trend. From the average cold gas efficiency point of view, the results displayed in Figure 5 show a higher performance for experiments carried out at λ = 35 %. These results can be explained considering that the yield to gas obtained, y_{gas}, increases with the equivalence ratio (see Table 4).

Figure 6 displays the tar productions based on the DSS fed as a function of the temperature and equivalence ratio. As can be seen, the tar production decreases as the temperature increases (especially for the highest equivalence ratio values). Nevertheless, unexpected results were obtained when analyzing the influence of the equivalence ratio on the tar generation. The increase with the equivalence ratio of the tar produced (for temperatures below 850 ºC) can be related to the fact that the experimental value of λ is set adjusting the solid flow rate. Thus, a reduction of the DSS flow rate reduces the amount of ash, where Ca and Mg are present and could promote the catalytic cracking of tar species[22] in the regions of the bed and freeboard, as has been reported by Miccio et al.[23]

In light of the experimental results corresponding to section I, the best operating conditions in order to minimize the tar formation are T = 850 ºC and λ = 30 % (run #I.6).

Two experimental runs (section II) were performed to analyze the influence of the fluidizing velocity on the gasification results. Figure 7 shows the tar generated and gas yield as a function of the ratio u / u_{mf} for the experiments #I.6, #II.1, and #II.2 (T = 850 ºC and λ = 30 % in all cases).

As can be observed in Figure 7, the tar generated at eight times u_{mf} was much lower than that obtained for any other fluidizing velocity studied. On the other hand, the specific yield to gas obtained in run #I.6 was unexpectedly low (see Table 4 for related LHV and η values). This result could be due to an underestimation of the total gas volume produced during the experiment #I.6.

Gasification tests using alumina as bed additive. Table 6 reports the results of gasification tests corresponding to section III (see Table 3).

The effect of the in-bed addition of alumina on gas composition is shown in Figure 8 for the experiments performed at T = 850 ºC and λ = 30 % (the best operating conditions for minimizing tar generation).

The H_2 content in the flue gas increases with the percentage of alumina added in the reactor. This increase is due to steam reforming and cracking reactions of the tar and light hydrocarbons present in the raw gas, both producing hydrogen,[24,25] and also to the CO shift reaction according to Orío et al.[26]

The CO content in the gas slightly increased with the proportion of alumina, as Figure 8 shows. The net result is a function of at least two simultaneous and competing reactions: steam reforming which generates CO and the water-shift reaction which consumes CO. On the other hand, the variation of the CO_2 content in the flue gas using alumina as a bed material is very small.

The methane content also increases slightly in the experiments performed. This result could again be due to two simultaneous types of reactions: steam and thermal cracking of tars, which can generate CH_4 from higher hydrocarbons, and CH_4 steam and CO_2 reforming reactions, which consume some CH_4 from the fuel gas.

As a result of changes in the gas composition, the heating value of the gas increases proportionally to the alumina added (see Figure 9). This increase of the LHV is mainly due to the fact that tars (not taken into account in the LHV of the gas) are converted into H_2 and CH_4, thus increasing the heating value of the gas produced.

Figure 10 displays the tar production based on the DSS fed as a function of the percentage of alumina added to the reactor (at T = 850 ºC and λ = 30 %). As can be expected, and in accordance with the gas composition results mentioned above, the tar production drastically decreases as the quantity of in-bed alumina increases, except for run #III.7 (this unexpected result needs to be analyzed and compared in future studies).

The tar content decreases by nearly 40 % with the in-bed use of alumina (5–6 % of DSS fed).

An additional gasification test (run #III.4) was carried out in order to analyze the results obtained at T = 850 ºC and λ = 25 %. As can be seen in Table 6, the performance corresponding to run #III.4 was worse than the tests performed at λ = 30 %.

Conclusions

Because limited information is available about sewage sludge gasification in a bubbling fluidized bed, the work presented here examines the effect of three important process variables (temperature, equivalence ratio, and fluidizing velocity) on several gasification parameters: the gas yield and composition, the average cold gas efficiency, and the tar content in the raw gas. These data are required in order to quantify the potential energy power of dried sewage sludge as well as to evaluate the optimum conditions for its gasification.

Overall, the results obtained are encouraging for the application of bubbling fluidized bed gasification with air as an option for energy recovery from sewage sludge. However, some unexpected results related to tar generation as a function of the equivalence ratio could be due to the effect of additional variables and gasification parameters. Further research is therefore needed in order to analyze the influence of, among others factors, the bed height, the particle size distribution, and the freeboard temperature.

In light of the high tar content in the raw gas, the in-bed use of alumina has been tested. This primary measure has proved effective in order to produce a gas of higher hydrogen content with lower tar content. However, these results should be considered as preliminary. Further investigations are in progress to check and develop other additives.

Acknowledgement

The authors would like to express their gratitude to J. Abrego and G. García for their excellent support in performing the experiments. J.J.M. acknowledges the postdoctoral grant received from the Spanish Ministry of Education and Science (MEC) and the European Social Found (ESF).

Nomenclature

BFB = bubbling fluidized bed

DSS = dried sewage sludge

daf = dry and ash free basis

LHV = lower heating value of the produced gas, dry basis

l_0 = litter, normal conditions (0 ºC, 101 kPa)

m_0^3 = cubic meter, normal conditions (0 ºC, 101 kPa)

Q_{air} = air flow rate used in an experiment, l_0/min

Q_{sludge} = mass flow rate of sewage sludge, g/min

T = bed temperature, ºC

u = superficial gas velocity at the inlet of the gasifier bed, cm/s

u_{mf} = minimum fluidization gas velocity (gasifier bed conditions), cm/s

y_{carbon} = average percentage of carbon in the biomass recovered in the gas

y_{gas} = specific yield to gas obtained, m_0^3 of dry gas / kg of daf DSS fed

Greek Symbols

η = average cold gas efficiency based on LHV of gas and biomass, %

λ = equivalence ratio, defined as the air-to-fuel ratio used in the reactor divided by the air-to-fuel ratio for the stoichiometric combustion, %

References

(1) Werther, J.; Ogada, T. *Prog. Energy Combust Sci.* **1999**, *25(1)*, 55–116.

(2) Midilli, A.; Dogru, M.; Howarth, C. R.; Ling, M. J.; Ayhan, T. *Energy Convers. Manage.* **2001**, *42*, 157–172.

(3) Winkler, M. *Chem. Ind. (London)* **1993**, *7*, 217–223.

(4) Lu, G. Q.; Low, J. C. F.; Liu, C. Y.; Lua; A. C. *Fuel* **1995**, *74(3)*, 344–348.

(5) Urban D. L.; Antal, M. J. *Fuel* **1982**, *61*, 799–806.

(6) Kaminsky, W.; Kunumer, A. B. *J. Anal. Appl. Pyrolysis* **1989**, *16*, 27–35.

(7) Stammbach, M. R.; Kraaz, B.; Hagenbuche, R.; Richarz, W. *Energy Fuels* **1989**, *3*, 255–259.

(8) Bellmann, U.; Kummer, A. B.; Ying, Y.; Kaminsky, W. In *Pyrolysis and Gasification*; Ferrero, G. L., Maniatis, K., Buekens, A., Bridgewater, A. V., Eds.; Elsevier Applied Science: London and New York, 1989; pp 190–194.

(9) Dumpelmann, R.; Richarz, W.; Stammbach, M. R. *Can. J. Chem. Eng.* **1991**, *69(4)*, 953–963.

(10) Bretchel, H.; Eipper, H. *Water Sci. Techol*. **1990**, *22(12)*, 169–276.

(11) Lowe, P.; Boutwood, J. *Alternative uses for sewage sludge*. Pergamon Press: Oxford, 1989; pp 277–284.

(12) Boocock, D. B. G.; Konar, S. M.; Makay, A.; Cheung, P. T. C.; Liu, J. *Fuel* **1992**, *71(11)*, 1291–1297.

(13) Konar, S. M.; Boocock, D. G. B.; Mao, V.; Liu, J. *Fuel* **1994**, *73(5)*, 642–646.

(14) Ramphorst, M. P.; Ringel, H. D. *J. Anal. Appl. Pyrolysis* **1994**, *28*, 137–155.

(15) Werther, J.; Saenger, M. *J. Chem. Eng. Jpn*. **2000**, *33*, 1–11.

(16) Bacaicoa, P. G.; Bilbao, R.; Uson, C. In *Proceedings of the Second Biomass Conference: Energy, Environment, and Agricultural Industry*, 1995; pp 685–694.

(17) Devi, L.; Ptasinski, K. J.; Janssen, F. J. J. G. *Biomass Bioenergy* **2003**, *24*, 125–140.

(18) Stevens D. J. Subcontract report NREL/SR-510-29952, National Renewable Energy Laboratory: Golden, Colorado, August 2001.

(19) Van Paasen S V. B.; Rabou L. P. L. M.; Bär R. In *Proceedings from the 2004 2nd World Conference and Technology Exhibition on Biomass for Energy, Industry and Climate Protection*, Rome, Italy.

(20) Narváez, I.; Corella, J.; Orío, A. *Ind. Eng. Chem. Res*. **1997**, *36*, 317–327.

(21) Aznar, M. P.; Caballero, M. A.; Gil, J.; Martín J. A.; Corella, J. *Ind. Eng. Chem. Res.* **1998**, *37*, 2668–2680.

(22) Bridgewater, A.V. *Fuel* **1995**, *74*, 631–653.

(23) Miccio, F.; Moersch, O.; Spliethoff, H.; Hein, K.R.G. In *Proceedings of the 15th International Conference on Fluidized Bed Combustion*. Reuther, R. B. Ed.; ASME: New York, 1999; pp 108–120.

(24) Zhang, Z.; Baerns, M. *Appl. Catal.* **1991**, *75*, 299–310.

(25) Simell, P. A.; Brendenberg, J. B. *Fuel* **1990**, 69, 1219–1225.

(26) Orío, A.; Corella, J.; Narváez, I. *Ind. Eng. Chem. Res.* **1997**, *36*, 3800–3808.

Table 1. Analysis of dried sewage sludge samples

Proximate	Analytical standard	% by weight
Moisture	ISO-589-1981	8.92
Ash	ISO-1171-1976	42.12
Volatiles	ISO-5623-1974	42.30
Fixed Carbon	By difference	6.66

Ultimate (organic fraction)	Analytical instrument	% by weight (daf)
Carbon	Carlo Erba 1108	55.33
Hydrogen	Carlo Erba 1108	6.70
Nitrogen	Carlo Erba 1108	8.15
Sulphur	Carlo Erba 1108	1.75
Oxygen	By difference	28.07

Table 2. Properties of Alumina (Spheralite 505)

Determinations	Results	Units
Particle size distribution. Sieve > 4 mm	0.5	%
Particle size distribution. Sieve < 2 mm	0.5	%
Tapped bulk density	693	kg/m^3
Surface area (BET)	281	m^2/g
Volume of pores < 8 μm	58.8	$cm^3/100$ g
Particle crushing strength	6.3	daN
Loss from 300 ºC to 1000 ºC	3.1	%
Na as Na_2O	701	ppm
Al_2O_3 / 1000 ºC	≥ 93.5	%

Table 3. Summary of operating conditions for the experiments

Test no.	Temperature (ºC)	λ (%)	Q_{sludge} (g/min)	Q_{air} (l_0/min)	u/u_{mf} (–)	Sand added (% of DSS fed)	Alumina added (% of DSS fed)
I.1	750	25	4.53	3.75	7.2	20	0
I.2	800	25	4.53	3.75	7.6	20	0
I.3	850	25	4.53	3.75	8.0	20	0
I.4	750	30	3.78	3.75	7.2	20	0
I.5	800	30	3.78	3.75	7.6	20	0
I.6	850	30	3.78	3.75	8.0	20	0
I.7	750	35	3.23	3.75	7.2	20	0
I.8	800	35	3.23	3.75	7.6	20	0
I.9	850	35	3.23	3.75	8.0	20	0
II.1	850	30	2.37	2.35	5.0	20	0
II.2	850	30	5.21	5.18	11.0	20	0
III.1	850	30	3.78	3.75	8.0	18	2
III.2	850	30	3.78	3.75	8.0	16	4
III.3	850	30	3.78	3.75	8.0	15	5
III.4	850	25	4.53	3.75	8.0	15	5
III.5	850	30	3.78	3.75	8.0	14	6
III.6	850	30	3.78	3.75	8.0	12	8
III.7	850	30	3.78	3.75	8.0	10	10

Table 4. Experimental results of gasification tests (section I and II)

Run no.	I.1	I.2	I.3	I.4	I.5	I.6	I.7	I.8	I.9	II.1	II.2
λ (%)	25.0	25.9	25.1	29.4	29.7	29.5	36.1	35.9	35.1	30.0	29.7
Temperature† (ºC)	750	800	850	750	800	850	750	800	850	850	850
Q_{sludge} (g/min)	4.53	4.36	4.52	3.85	3.82	3.84	3.14	3.15	3.23	2.36	5.26
Q_{air} (l_0/min)	3.75	3.75	3.75	3.75	3.75	3.75	3.75	3.75	3.75	2.35	5.18
Average gas composition (% vol. dry basis)											
H_2	4.48	5.06	6.06	3.65	4.03	4.41	3.71	3.11	3.26	5.20	4.61
O_2	0.01	0.00	0.00	0.01	0.01	0.01	0.01	0.13	0.01	0.04	0.00
N_2	67.97	66.62	63.94	70.10	68.37	67.54	69.24	69.05	69.09	65.53	65.54
CO	7.95	7.95	8.60	6.91	6.98	7.80	6.73	6.97	7.56	7.87	8.49
CH_4	2.17	2.27	2.65	1.59	1.91	2.20	1.84	1.87	2.06	2.65	2.58
CO_2	16.35	16.52	15.95	16.39	16.63	15.71	16.75	16.49	15.70	16.35	16.05
C_2H_4	0.51	1.04	2.23	0.88	1.68	1.93	1.37	2.04	1.94	1.94	2.19
C_2H_6	0.05	0.08	0.14	0.05	0.07	0.07	0.10	0.07	0.05	0.03	0.05
C_2H_2	0.14	0.14	0.18	0.13	0.13	0.14	0.07	0.13	0.20	0.21	0.24
H_2S	0.35	0.32	0.23	0.29	0.19	0.19	0.17	0.13	0.13	0.18	0.24
y_{gas} (m_0^3/kg of daf DSS)	1.96	2.08	2.10	2.25	2.31	2.33	2.78	2.78	2.72	2.45	2.43
LHV (kJ/m_0^3)	2684	3110	4205	2462	3114	3507	2821	3211	3332	3785	3952
η (%)	25.2	30.9	42.1	26.3	34.4	39.1	37.5	42.6	43.2	44.2	45.8
y_{carbon} (%)	48.5	53.0	65.4	51.5	63.3	66.2	67.7	75.7	76.6	74.1	75.9
Product distribution based on the sludge fed (% weight)											
Gas	49.1	52.8	54.7	51.6	53.1	55.8	58.6	60.8	64.7	64.1	64.9
Tar	7.0	6.6	5.6	9.9	8.1	4.8	11.5	10.7	6.5	9.0	8.4
Water	23.4	18.3	21.3	20.3	21.3	21.7	17.3	16.8	17.1	16.3	16.2
Product distribution based on the sludge and air fed (% weight)											
Gas	39.4	42.0	43.8	40.0	41.0	43.1	43.1	44.8	48.0	49.4	50.1
Char	33.7	33.5	33.7	32.6	32.5	32.6	31.0	31.0	31.2	32.4	32.5
Tar	5.6	5.6	4.5	7.7	6.2	3.7	8.5	7.9	4.9	7.0	6.5
Water	18.7	14.5	17.0	15.7	16.5	16.8	12.7	12.4	12.7	12.6	12.5
TOTAL	97.4	95.3	99.0	96.0	96.2	96.2	95.3	96.1	96.7	101.3	101.6

† Temperature of the fluidized bed. For all experiments performed in this study, the temperature set-points corresponding to the freeboard and cyclone were 600 ºC and 350 ºC, respectively.

Table 5. Reproducibility of experimental results (gasification run #I.6)

Run no.	I.6	I.6b	I.6c
λ (%)	29.5	29.9	29.8
Temperature (ºC)	850	850	850
Q_{sludge} (g/min)	3.84	3.78	3.80
Q_{air} (l_0/min)	3.75	3.75	3.75
Average gas composition (% vol. dry basis)			
H_2	4.41	4.28	4.33
O_2	0.01	0.00	0.00
N_2	67.54	67.42	67.47
CO	7.80	7.95	7.76
CH_4	2.20	2.22	2.19
CO_2	15.71	15.75	15.79
C_2H_4	1.93	1.93	1.91
C_2H_6	0.07	0.10	0.09
C_2H_2	0.14	0.14	0.13
H_2S	0.19	0.20	0.18
y_{gas} (m_0^3/kg of daf DSS)	2.33	2.29	2.33
LHV (kJ/m_0^3)	3507	3544	3487
η (%)	39.1	40.1	39.3
y_{carbon} (%)	66.2	68.0	67.7
Product distribution based on DSS fed (% weight)			
Gas	55.8	56.8	55.0
Tar	4.8	5.1	5.2
Water	21.7	21.4	21.0
Product distribution based on DSS and air fed (% weight)			
Gas	43.1	43.8	42.4
Char	32.6	32.5	33.0
Tar	3.7	3.9	4.0
Water	16.8	16.5	16.2
TOTAL	96.2	96.7	95.6

Table 6. Experimental results of gasification tests using alumina (section III)

Run no.	III.1	III.2	III.3	III.4	III.5	III.6	III.7
λ (%)	31.0	30.4	30.2	24.5	30.5	30.1	29.4
Temperature (ºC)	850	850	850	850	850	850	850
Q_{sludge} (g/min)	3.65	3.72	3.75	4.62	3.72	3.76	3.85
Q_{air} (l_0/min)	3.75	3.75	3.75	3.75	3.75	3.75	3.75
Average gas composition (% vol. dry basis)							
H_2	6.14	6.47	7.98	8.77	8.37	8.67	8.81
O_2	0.01	0.01	0.00	0.01	0.17	0.00	0.00
N_2	65.57	65.60	63.27	61.72	63.15	62.69	61.83
CO	8.01	7.99	8.57	9.21	8.63	8.81	8.96
CH_4	2.16	2.08	2.24	2.39	2.17	2.20	2.35
CO_2	15.94	15.83	15.81	15.67	15.48	15.61	15.89
C_2H_4	1.81	1.67	1.76	1.88	1.68	1.69	1.76
C_2H_6	0.05	0.04	0.07	0.06	0.07	0.04	0.07
C_2H_2	0.12	0.10	0.09	0.10	0.09	0.09	0.12
H_2S	0.20	0.20	0.21	0.20	0.20	0.20	0.20
y_{gas} (m_0^3/kg of daf DSS)	2.53	2.47	2.55	2.12	2.57	2.57	2.53
LHV (kJ/m_0^3)	3609	3520	3877	4168	3848	3909	4075
η (%)	43.6	41.6	47.2	42.2	47.4	47.9	49.5
y_{carbon} (%)	71.3	69.4	72.7	63.5	73.6	74.7	74.4
Product distribution based on the sludge fed (% weight)							
Gas	59.5	59.3	60.2	53.6	63.4	64.8	61.8
Tar	4.3	3.8	3.0	4.4	2.8	2.7	4.1
Water	20.6	19.8	19.7	18.6	20.3	19.9	15.9
Product distribution based on the sludge and air fed (% weight)							
Gas	45.5	45.5	46.3	43.1	48.7	49.8	47.8
Char	32.2	32.3	32.4	33.9	32.3	32.4	32.6
Tar	3.3	2.9	2.3	3.5	2.2	2.1	3.2
Water	15.7	15.2	15.2	14.9	16.0	15.3	12.3
TOTAL	96.7	96.0	96.2	95.5	99.1	99.6	95.9

Caption for Figures

Figure 1. Fluid Bed Reactor system: 1. Air; 2. Air Mass Flow Controller; 3. Rotameters; 4. Manometers; 5. Variable frequency driver; 6. Screw feeder; 7. Feed hopper; 8. Air inlets; 9. Cooling Air; 10. Fluid Bed Reactor; 11. Cyclone; 12. "Char pot"; 13. Ash hopper; 14. K thermocouples; 15. Temperature Controller; 16. Tar condensers; 17. Cotton Filter; 18. CO/CO_2 Analyzer; 19. Volumetric Gas meter.

Figure 2. Evolution of the gas composition during run #I.6 (▽, CO_2; ●, CO; □, H_2; ▲, CH_4; ○, C_2H_4; ★, C_2H_6; ◇, C_2H_2; +, H_2S).

Figure 3. Average gas composition for the experiments performed in section I as a function of temperature (a) and equivalence ratio (b): □, H_2; ●, CO; ▽, CO_2; ✳, N_2; ▲, CH_4; ○, C_2H_4; ★, C_2H_6; ◇, C_2H_2; +, H_2S; ⧋, O_2.

Figure 4. Evolution of LHV *versus* temperature (runs I.1–I.9) for the different equivalence ratios studied (λ: ●, 25%; □, 30%; △, 35%).

Figure 5. Evolution of η *versus* temperature (runs I.1–I.9) for the different equivalence ratios studied (λ: ●, 25%; □, 30%; △, 35%).

Figure 6. Tar production (runs I.1–I.9) as a function of the temperature and the equivalence ratio (λ: □, 25%; ■, 30%; ◪, 35%).

Figure 7. Evolution of the tar generation and gas yield *versus* the ratio u / u_{mf} (◆, tar; □, y_{gas}).

Figure 8. Mean gas composition as a function of alumina added to the gasifier. **(a)**: □, H_2; ●, CO; ▽, CO_2; ✳, N_2. **(b)**: ▲, CH_4; ○, C_2H_4; ★, C_2H_6; ◇, C_2H_2; +, H_2S; ⧋, O_2.

Figure 9. Variation of LHV and η as a function of alumina added to reactor (◆, LHV; □, η).

Figure 10. Evolution of the tar content *versus* the percentage of alumina added to the reactor.

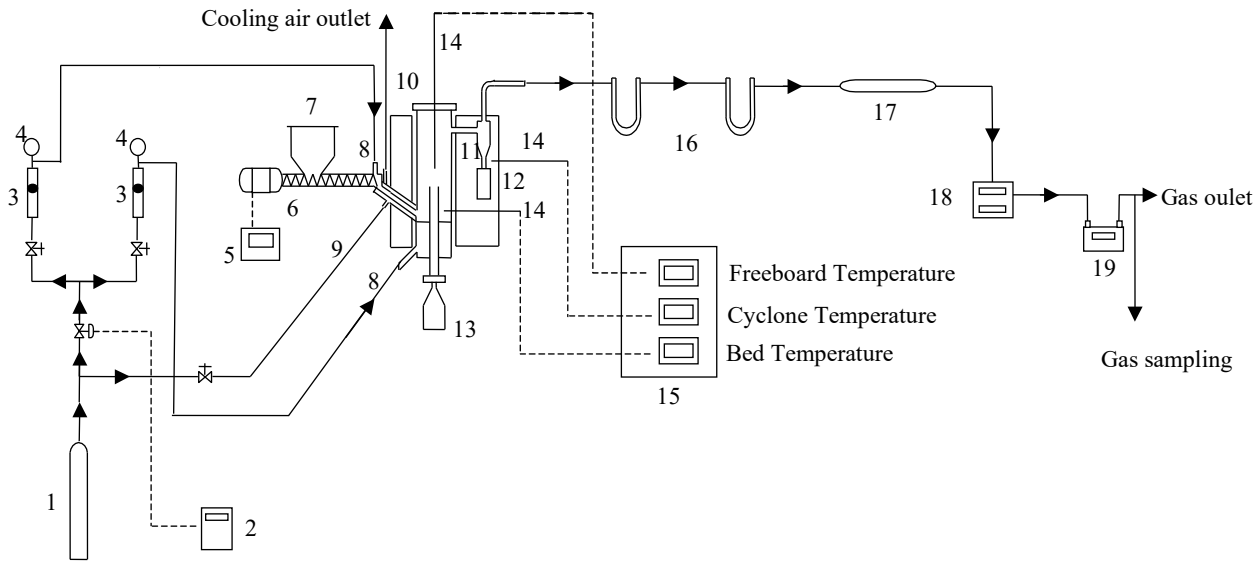
Cooling air outlet
14
10
7
4
4
8
11
14
16
17
3
3
6
12
14
18
Gas oulet
5
9
19
8
Freeboard Temperature
Cyclone Temperature
Bed Temperature
13
Gas sampling
15
1
2

Figure 1

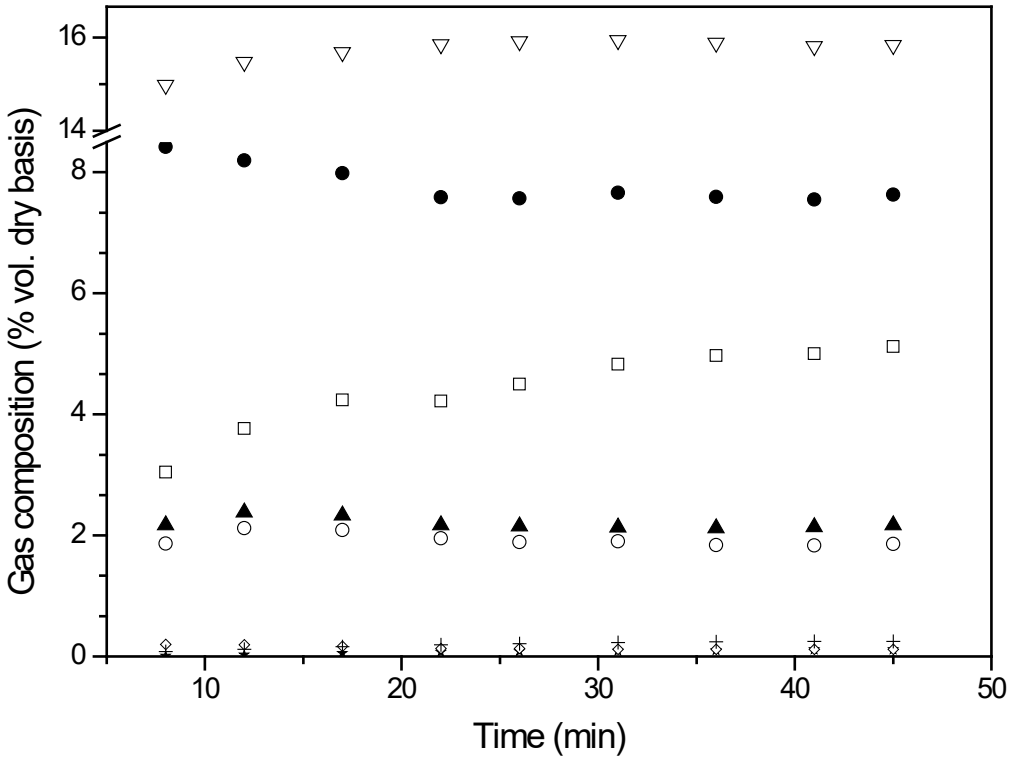
Gas composition (% vol. dry basis)
16
14
8
6
4
2
0
10
20
30
40
50
Time (min)

Figure 2

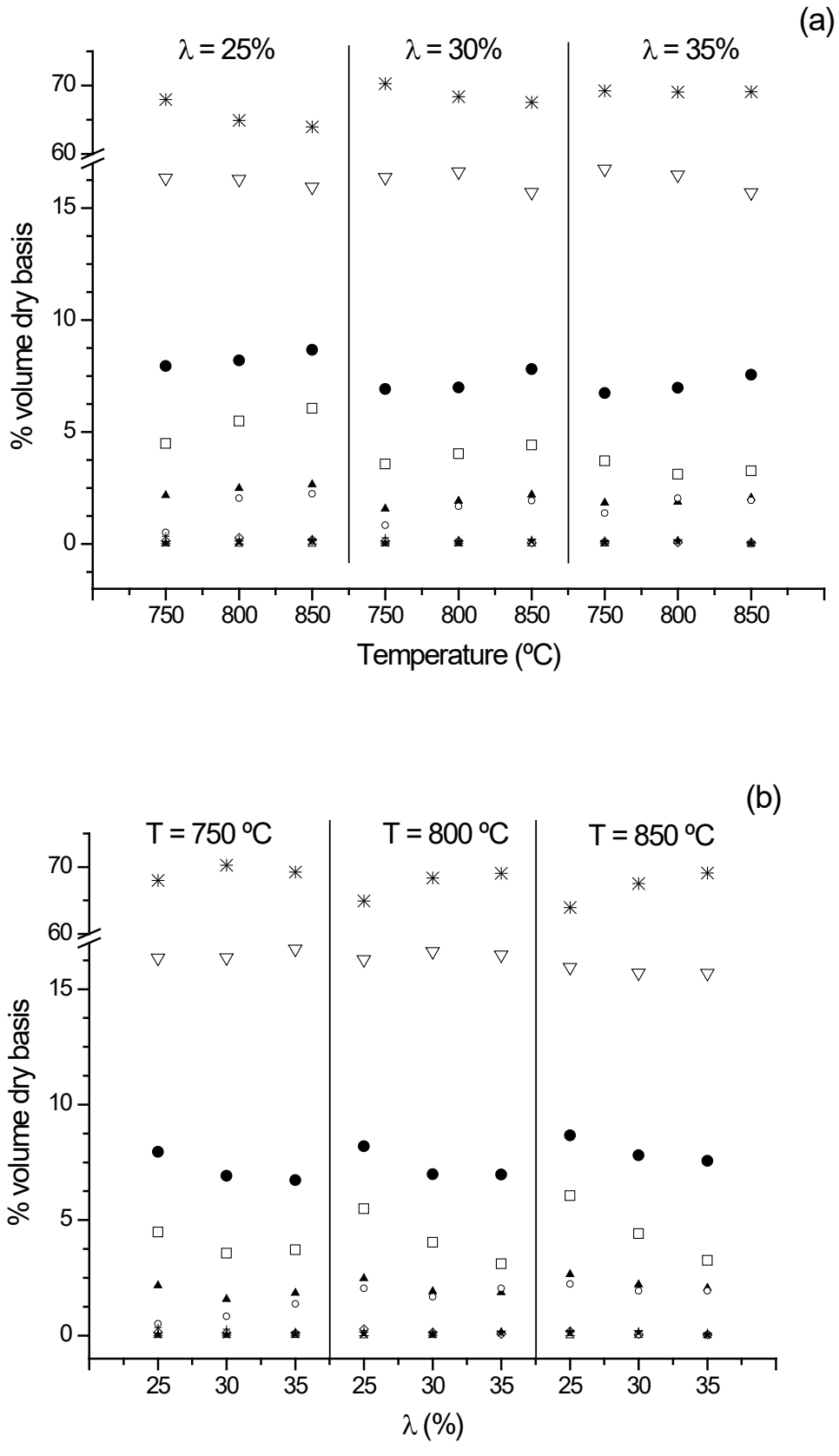
(a)
λ = 25%
λ = 30%
λ = 35%
% volume dry basis
70
60
15
10
5
0
750
800
850
Temperature (ºC)
(b)
T = 750 ºC
T = 800 ºC
T = 850 ºC
25
30
35
λ (%)

Figure 3

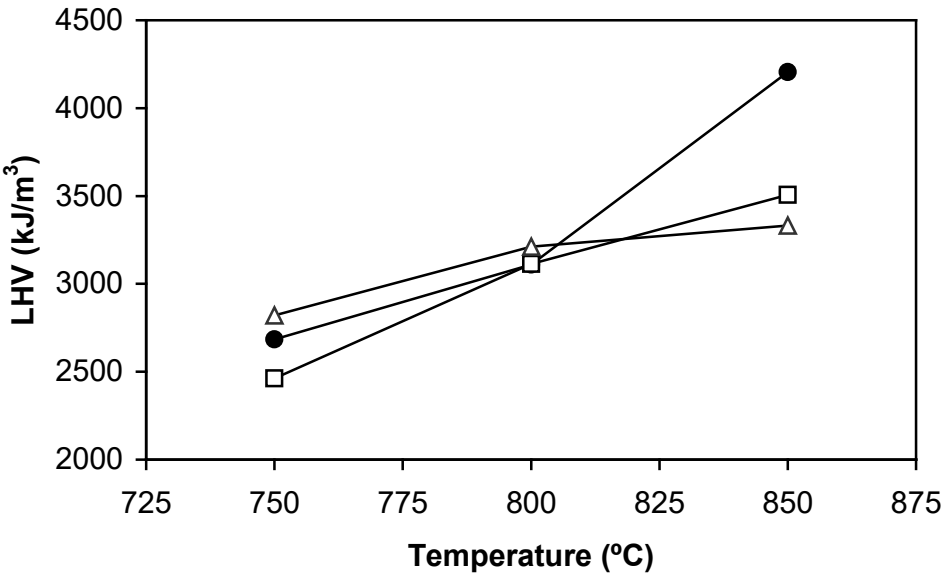
4500
4000
3500
3000
2500
2000
LHV (kJ/m3)
725
750
775
800
825
850
875
Temperature (ºC)

Figure 4

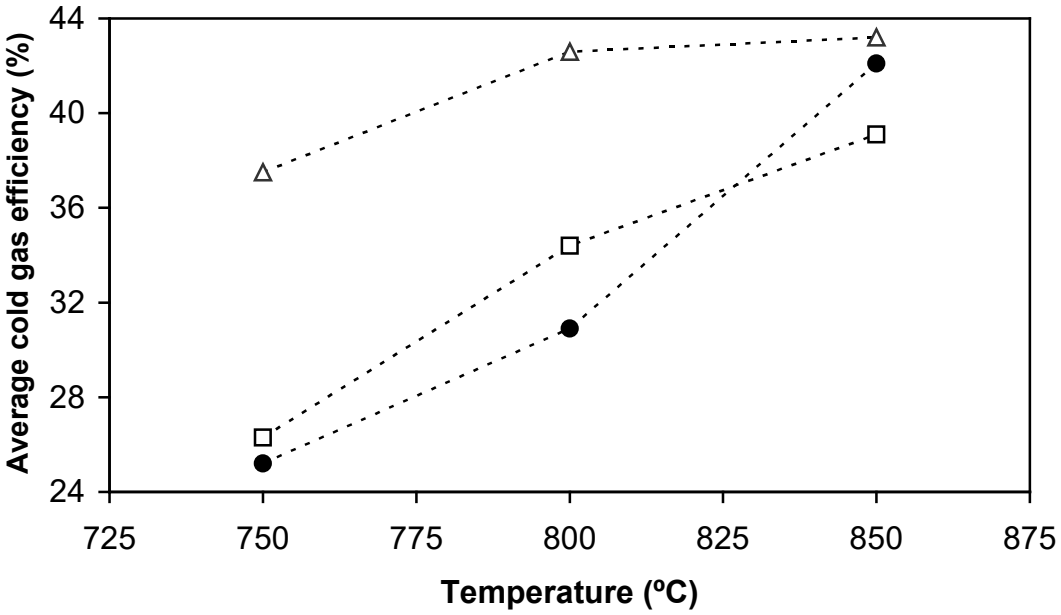
Average cold gas efficiency (%)
44
40
36
32
28
24
725
750
775
800
825
850
875
Temperature (ºC)

Figure 5

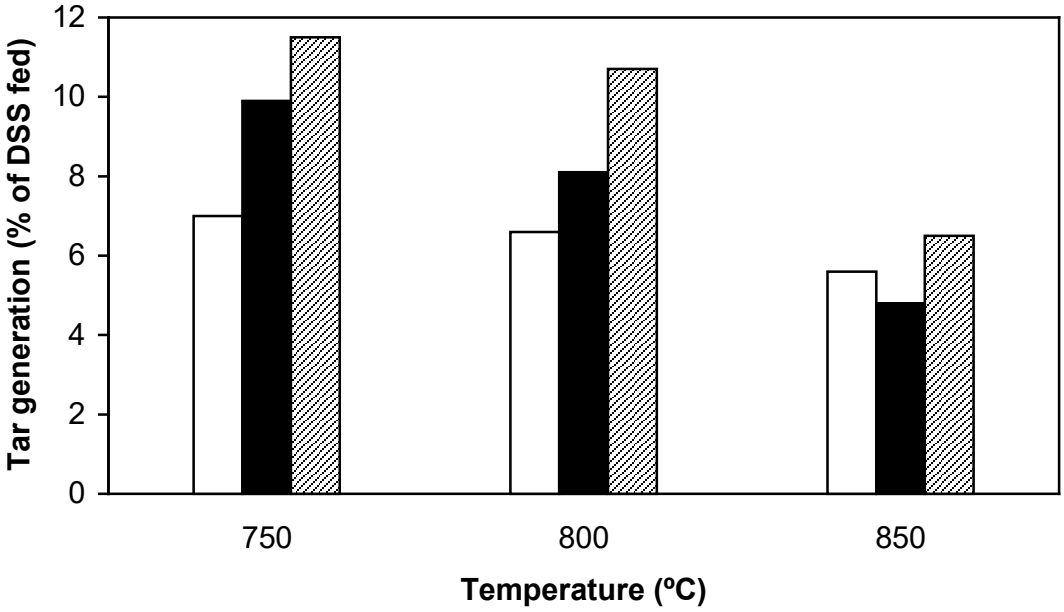
Tar generation (% of DSS fed)
12
10
8
6
4
2
0
750
800
850
Temperature (ºC)

Figure 6

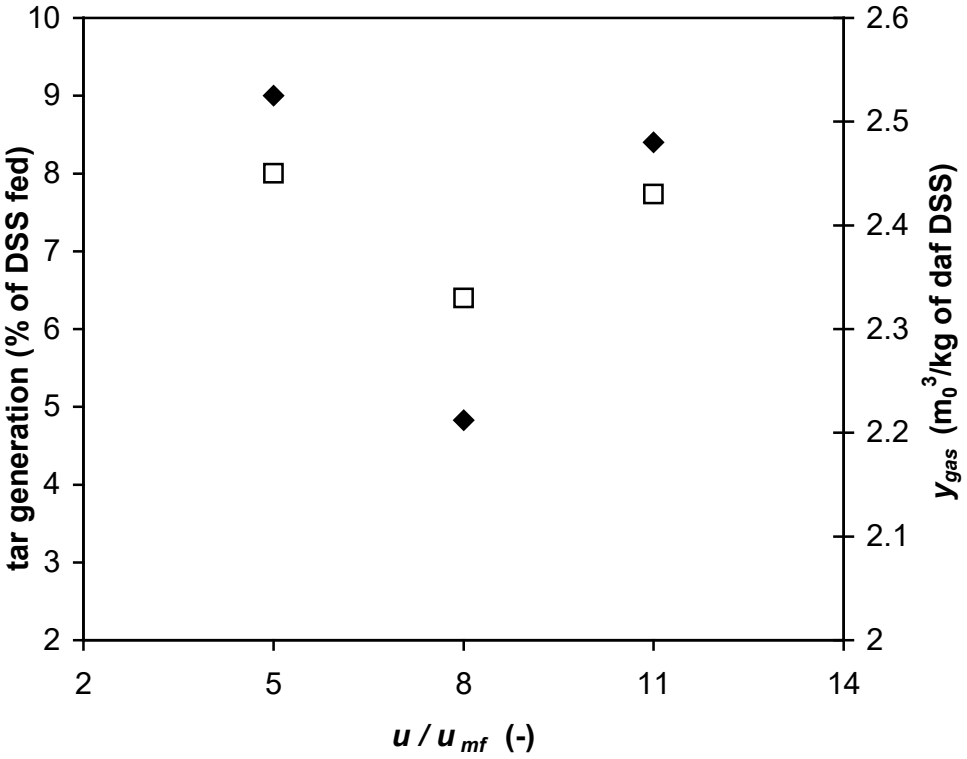
10
9
8
7
6
5
4
3
2
2.6
2.5
2.4
2.3
2.2
2.1
2
2
5
8
11
14
tar generation (% of DSS fed)
y_{gas} (m_0^3/kg of daf DSS)
u / u_{mf} (-)

Figure 7

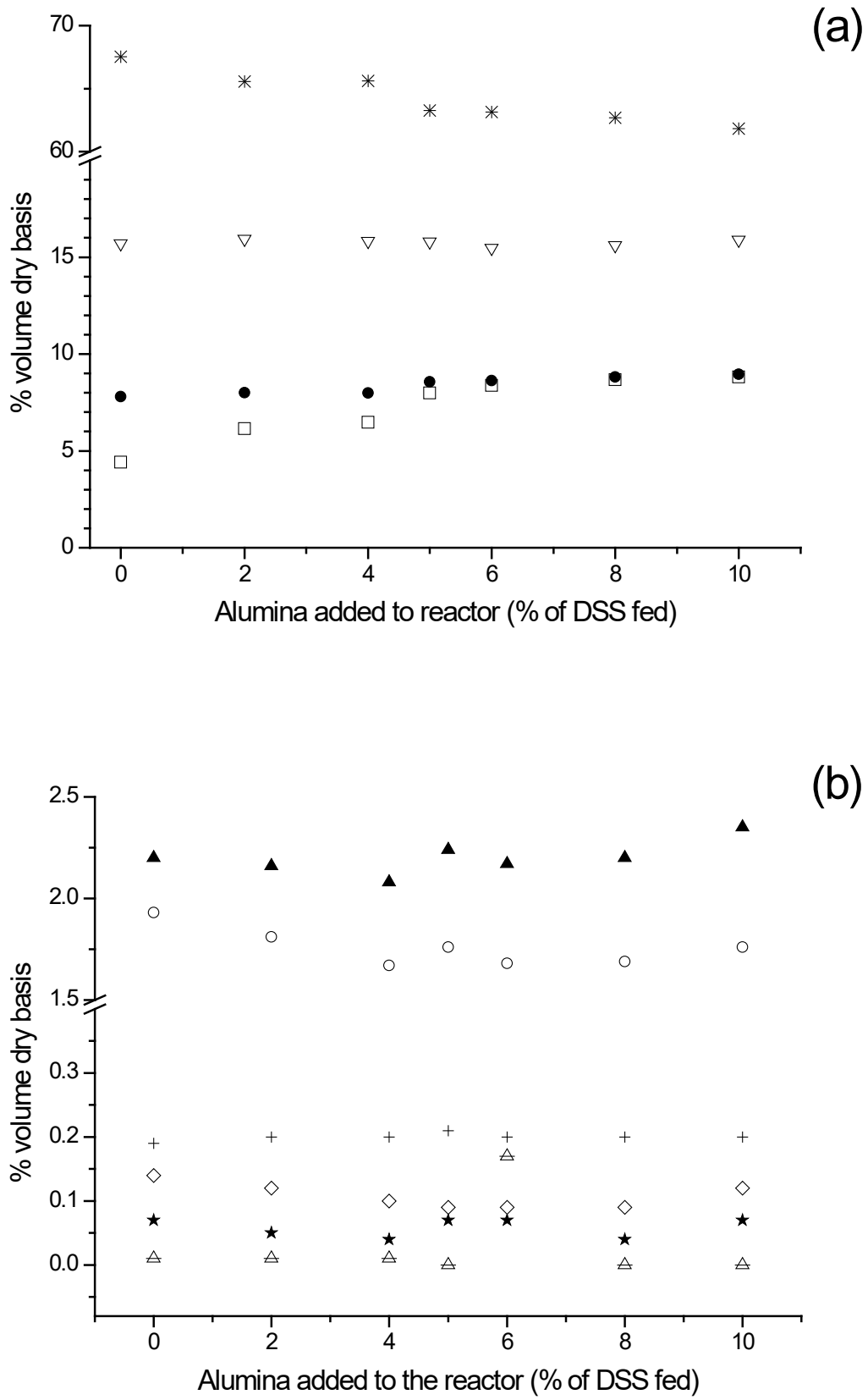
(a)
70
60
15
10
5
0
% volume dry basis
0
2
4
6
8
10
Alumina added to reactor (% of DSS fed)
(b)
2.5
2.0
1.5
0.3
0.2
0.1
0.0
% volume dry basis
0
2
4
6
8
10
Alumina added to the reactor (% of DSS fed)

Figure 8

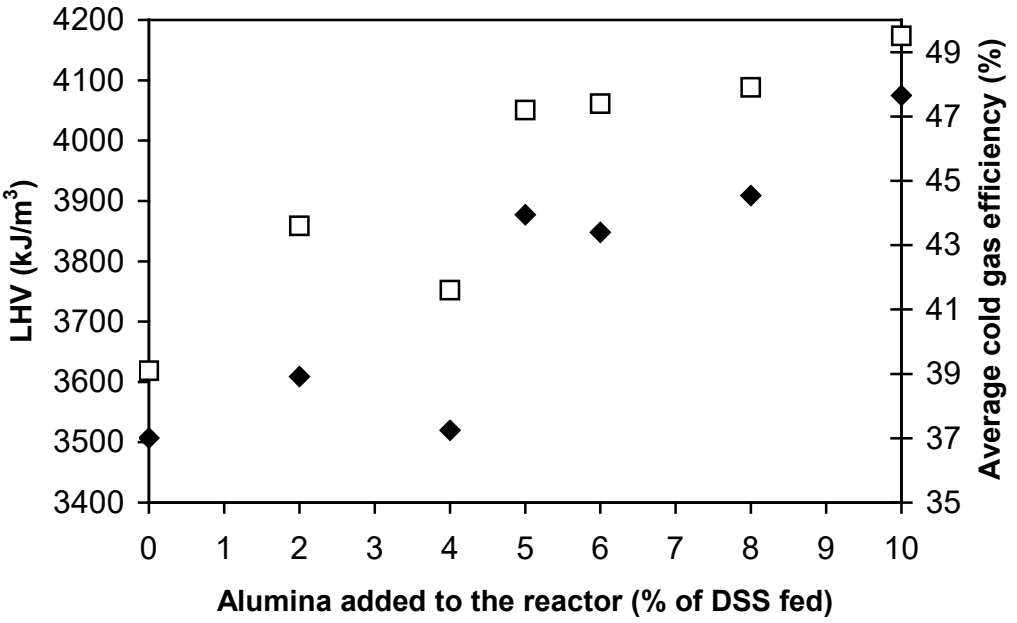
LHV (kJ/m3)
Average cold gas efficiency (%)
Alumina added to the reactor (% of DSS fed)
4200
4100
4000
3900
3800
3700
3600
3500
3400
49
47
45
43
41
39
37
35
0
1
2
3
4
5
6
7
8
9
10

Figure 9

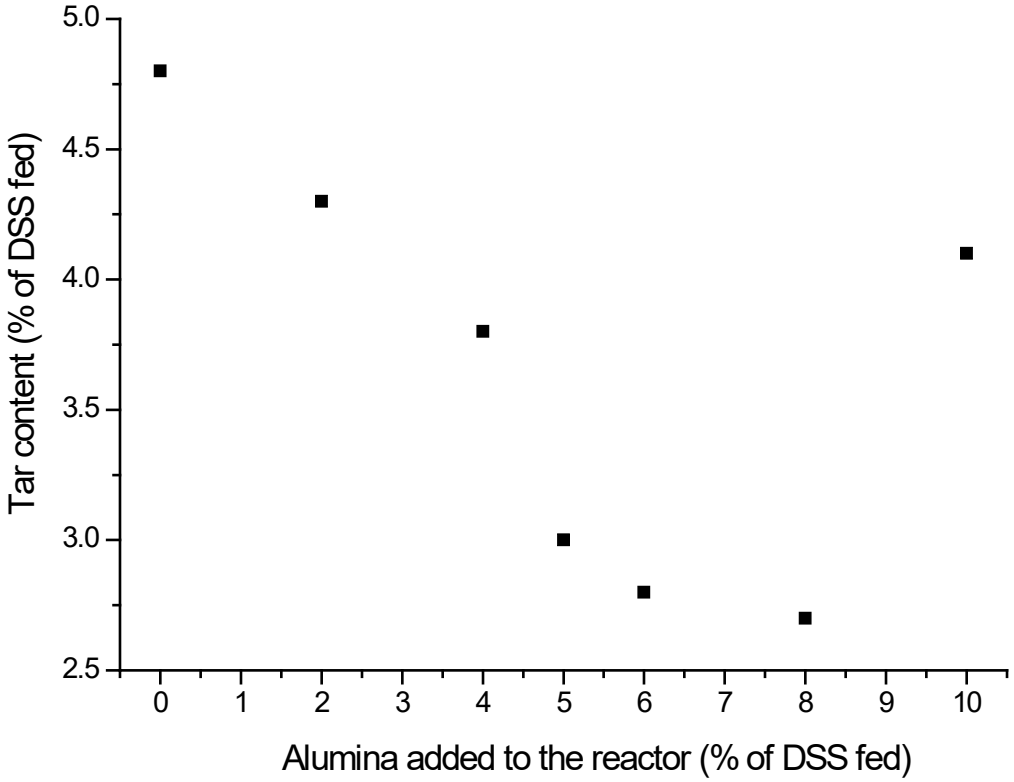
Tar content (% of DSS fed)
5.0
4.5
4.0
3.5
3.0
2.5
0
1
2
3
4
5
6
7
8
9
10
Alumina added to the reactor (% of DSS fed)

Figure 10